Available online at www.sciencedirect.com

ScienceDirect

Ceramics International 34 (2008) 599–604

CERAMICS INTERNATIONAL

www.elsevier.com/locate/ceramint

Densification and microwave dielectric properties of $CaO–B_2O_3–SiO_2$ system glass–ceramics

Chuang-Chung Chiang [a], Sea-Fue Wang [a,*], Yuh-Ruey Wang [a], Wen-Cheng J. Wei [b]

[a] Department of Materials and Mineral Resources Engineering, National Taipei University of Technology, 1, Sec. 3, Chung-Hsiao E. Rd., Taipei 106, Taiwan, ROC

[b] Department of Materials Science and Engineering, National Taiwan University, Taipei 106, Taiwan, ROC

Received 4 September 2006; received in revised form 11 December 2006; accepted 21 December 2006
Available online 30 January 2007

Abstract

In order to relieve the narrow processing window and poor material compatibility in practical applications as well as understand the microwave dielectric properties, investigation on the formulations of $CaO/B_2O_3/SiO_2$ glasses on their structure, thermal properties, and microwave properties were performed in this study. Six glasses with different molar ratios of $CaO/B_2O_3/SiO_2$ (designed as CBS-3, CBS-5, CBS-7, CBS-8, CBS-9, and CBS-10) were prepared and pulverized. Results indicate that most softening points of glasses are ranging from 680 to 710 °C. They were sintered at different temperatures to reach maximum densification. Among various glass formulations, CBS-9 glass–ceramic containing the largest amount of SiO_2 has the lowest CTE. The dielectric constants can be divided into two groups including around 4–5 and 7–8, and the dielectric losses (tan δ) are all below 0.005 in the frequency of $\approx$10 GHz. The dielectric constants and dielectric losses are generally frequency dependent. For CBS-9 glass–ceramic, the dielectric constant and dielectric loss at 4.7 and 18.6 GHz are 4.13 and 0.0018, and 4.20 and 0.0063, respectively.

Keywords: Glass–ceramics; LTCC; Microwave properties; $CaO–B_2O_3–SiO_2$

---

1. Introduction

In additional to the conventional printed circuit board technology, low-temperature co-firable ceramic (LTCC) technology is one of the new technologies to manufacture integrated multifunctional electronic chips [1]. It can be utilized for the integration of passive components into a monolithic, high reliable and robust LTCC module. These modules consist of several layers of substrate material with buried components such as capacitors, inductors, resistors, resonators, and filters. They are interconnected with 3D stripline circuitry. Utilization of low dielectric constant (K) LTCC substrate materials and associated high conductivity metallizations such as Au and Ag was found to have potential applications in the area of wireless communication [2].

A targeted LTCC substrate materials should possess several characteristics such as low dielectric constant and dielectric loss, high thermal conductivity, low thermal expansion coefficient (close to Si and GaAs), very robust against environmental stress, and low cost. LTCC substrate materials usually contain multiple phases. The properties of the multiphase systems not only depend on the properties and the extent of each phase present, but also the morphology, continuity, and connectivity of each phase [3,4]. In fabrication of desirable LTCC substrates, a complete densification and sufficient crystallization are generally necessary for the required mechanical properties and dielectric properties such as high Q value. Porosity and low degree of crystallinity would lead to relatively poor mechanical properties, and residual glass would detrimental to the Q value at microwave frequency. Approaches to achieve the above requirements are the use of binary glass systems including a high softening point glass and a low softening glass, nucleating agents, sintering aids, and properties and structure modifiers [5–8].

Among several LTCC glass–ceramic systems [6,9–11], $CaO–B_2O_3–SiO_2$ system has been reported as a promising material for use in microelectronic packaging because of low firing temperature and low dielectric loss [12,13]. Commercial

---

* Corresponding author.
E-mail address: seafuewang@yahoo.com (S.-F. Wang).

0272-8842/$34.00 © 2007 Elsevier Ltd and Techna Group S.r.l. All rights reserved.
doi:10.1016/j.ceramint.2006.12.008

available Ferro A6 LTCC system is a typical example. However, utilization of CaO–B_2O_3–SiO_2 glass–ceramic as LTCC substrate often encountered obstacles including narrow process window that is sensitive to firing profile and atmosphere, poor compatibility with the metallizations such as silver, and limited compatible materials for RLC components. Though crystallizations and physical properties of some specific CaO–B_2O_3–SiO_2 compositions were discussed in the literature, rare information regarding the compositional effects on the physical properties, particularly for microwave dielectric properties, of the CaO–B_2O_3–SiO_2 glass–ceramics have been reported. Optimization of glass–ceramic composition and further understanding of the structure–property relations of the CaO–B_2O_3–SiO_2 glass–ceramics for LTCC applications are required to relieve the obstacles encountered in practical applications. In this study, the effects of the compositions of CaO–B_2O_3–SiO_2 glass–ceramics on their thermal behaviors and microwave dielectric properties were systematically investigated and discussed.

2. Experimental procedure

The design of the glass compositions in this study is based on the phase diagram of CaO–B_2O_3–SiO_2 system [14], and the formulations are marked in Fig. 1, in which the CaO, B_2O_3, and SiO_2 are ranging from 10 to 70%, 7 to 32%, and 14 to 67%, respectively. Glasses of CaO–B_2O_3–SiO_2 system were prepared using the solid-state reaction technique, with high purity (>99.9% pure) of SiO_2, B_2O_3, and CaO (Wako, Reagent grade) as raw materials. Mixtures based on the weight percentages shown in Table 1 were mixed and milled in methyl alcohol solution using polyethylene jars and zirconia balls for 2 h and then oven-dried overnight at 80 °C. After drying, the powders were melt in an alumina crucible at the temperatures ranging from 1500 to 1650 °C for 1 h, depending on the glass composition. To prevent the occurrence of any crystallization, the melt was quenched into the de-ion water. Subsequently, the glasses were then crushed in the mortar and pestle and then re-milled in methyl alcohol for 10 h. Though some glasses have phase separation during melting, homogeneous distribution of the species was ensured through the milling. The pulverized glass powders were then subjected to particle size analysis and phase analysis using X-ray diffraction (XRD, Rigaku DMX-2200) with Cu Kα radiation to confirm their amorphous nature. Differential thermal analysis (DTA) was performed using Perkin-Elmer calorimeter, Series 1700 DTA, on the glasses to evaluate the possible reactions during heating.

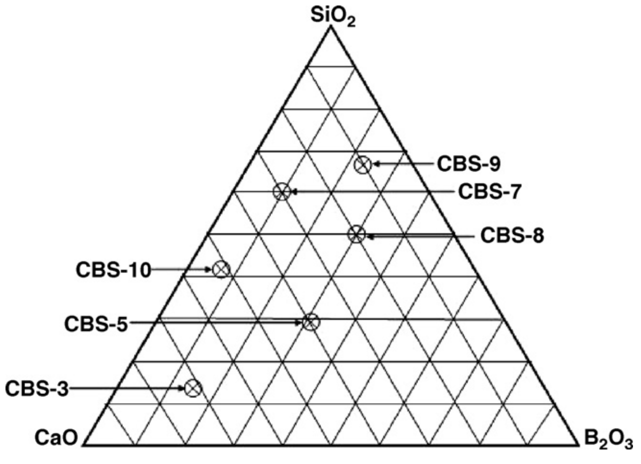

Fig. 1. The formulation design in this study.

Table 1
The formulations of various CaO–B_2O_3–SiO_2 glass–ceramics

Formulation	CaO		B_2O_3		SiO_2	
	mol%	wt%	mol%	wt%	mol%	wt%
CBS-3	69.7	66.4	16.2	19.2	14.1	14.4
CBS-5	38.3	34.9	31.5	35.6	30.2	29.5
CBS-7	29.3	27.5	9.3	10.8	61.4	61.7
CBS-8	19.8	17.8	30.9	34.6	49.3	47.6
CBS-9	10.5	9.5	22.2	25.0	67.3	65.5
CBS-10	50.1	47.8	7.3	8.6	42.6	43.6

The powder was added with a 5 wt% of 15%-PVA solution and pressed into disc-shaped compacts using uniaxial pressure of 1 t/cm^2. The samples were then heat treated at 550 °C for 2 h to eliminate the PVA, followed by sintering at temperatures between 800 and 925 °C for 15 min with a heating rate of 5 °C/min. In order to understand the effects of glass compositions on the sintering characteristic, dilatometric analyses were performed to characterize the shrinkage of the glass with respect to temperature. Experiments were performed using a DIL 402C dilatometer in air and at a heating rate of 5 °C/min. This method makes it possible to trace the onset temperature of the densification during sintering.

Density measurements were done using a liquid displacement method, with water as a media. Phase identification on the sintered glass–ceramics was performed using XRD. Scanning electron microscopy (SEM, Hitachi S4700), and energy dispersive spectroscopy (EDS) studies were used to reveal the microstructures of sintered samples. The normal (z) components of the dielectric constants (ε_r) and dielectric losses ($\tan\delta$) of the glass–ceramics values at microwave frequencies were measured in the TM_{010} mode using a Damaskos Model 400 [15] with a network analyzer (HP 8722ES). A cylindrical shaped unmetallized sample with an aspect ratio (diameter/height) $\gg 1$ was used to chock off many interfering modes. The sample was positioned inside the circular cavity with good contact to top and bottom plates. Dielectric constant and $\tan\delta$ were calculated from the frequency of the TM_{010} resonant mode.

3. Results and discussion

3.1. Densification behavior

The sintering shrinkage curves of the CaO–B_2O_3–SiO_2 powder compacts measured using dilatometer are revealed in Fig. 2. The densification behaviors of these systems behave differently due to their significant dissimilarity in the molar ratios of CaO/B_2O_3/SiO_2. The glass softening points obtained from DTA measurement are summarized in Table 2, which are also

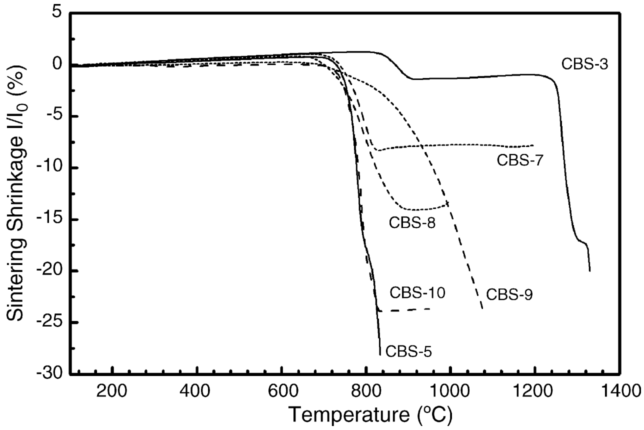

Fig. 2. Sintering shrinkage curves of the CaO–B_2O_3–SiO_2 powder compacts measured using dilatometer.

evident in the sintering shrinkage curves. The results indicate that most glass softening points are ranging from 680 to 710 °C, except CBS-3 at 830 °C. At the temperatures above the glass softening point, the viscous flow causes the shrinkage of glass (Fig. 2).

The level of the shrinkage is correlated to the locations of the glass softening point and the crystallization point [16]. The formation of the crystalline phase in the early stage generally retards the densification. Among the six compositions, CBS-3, containing rich CaO, has the highest onset temperature of the shrinkage and the smallest dimensional change, due to its high melting point (≈1400 °C). CBS-3 starts to crystallize at ≈920 °C, which ceases the densification and leads to the shrinkage concluding at less than 5%.

Both CBS-5 and CBS-10 follow a similar densification path and have a substantial shrinkage of over 20% below 800 °C and, afterward, the shrinkage of CBS-10 levels off. This is due to the facts that CBS-10 starts to crystallize $CaSiO_3$ above 800 °C, and CBS-5 has the lowest melting point (≈980 °C) among the systems in the phase diagram. CBS-10 has an exothermic peaks at temperatures around 820 °C, which is corresponding to the formation of $CaSiO_3$. CBS-7 and CBS-8 have a similar shrinkage route in the early stage of sintering. However, the densification of CBS-7 ended in 8% of shrinkage at 840 °C and CBS-8 concluded in a 14% of shrinkage at ≈870 °C. This is due to the crystallization process, which causes the expansion of the matrix. Though the above systems show different percentages of sintering shrinkage in Fig. 2, high densification was achieved based on the SEM micrographs shown in Fig. 3. Particularly, microstructures of CBS-5 and CBS-9 evidently indicate almost no porosity.

Fig. 4 shows the sintering densities of the CaO–B_2O_3–SiO_2 system glass–ceramics and Fig. 5 shows the XRD patterns of

Table 2
Physical properties of various CaO–B_2O_3–SiO_2 glass–ceramics

Formulation	Glass softening point (°C)	Thermal expansion coefficient ($\times 10^{-6}$ °C^{-1}) (from 25 to 500 °C)	Measuring frequency (GHz)	Dielectric constant	Dielectric loss	Temperature coeff. of dielectric constant (ppm/°C; at 10 kHz)
CBS-3	830	8.7	9.59	7.3	0.0041	52
CBS-5	705	8.2	9.59	7.3	0.0045	1690
CBS-7	700	7.3	9.97	3.9	0.0055	530
CBS-8	680	6.4	9.93	4.1	0.0048	214
CBS-9	710	3.5	9.92	4.1	0.0038	127
CBS-10	710	9.3	9.55	7.9	0.0045	29

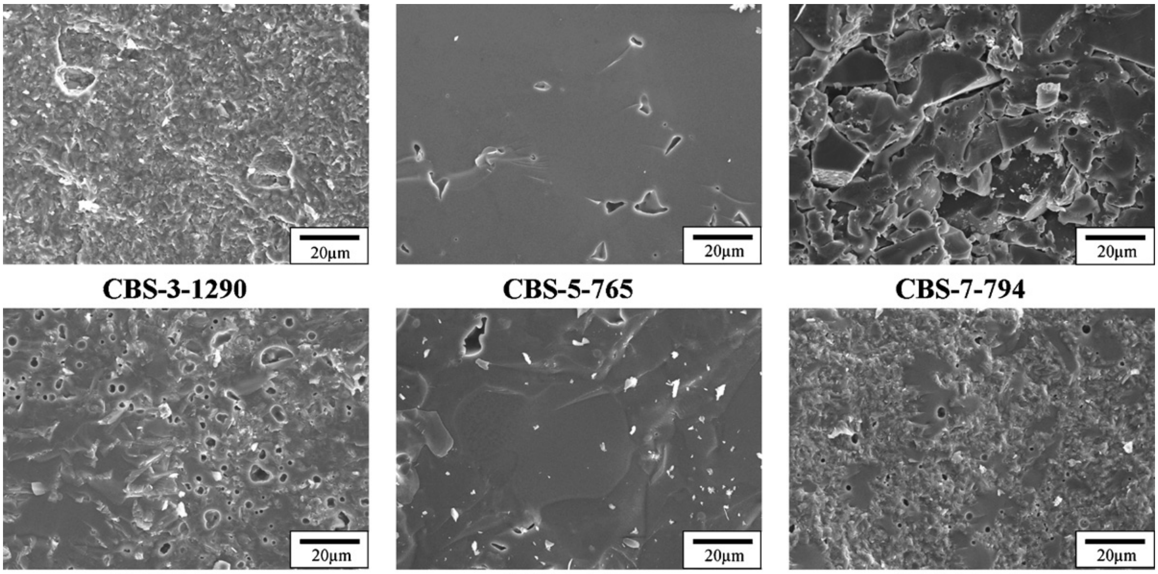

CBS-3-1290 **CBS-5-765** **CBS-7-794**

CBS-8-900 **CBS-9-1050** **CBS-10-800**

Fig. 3. SEM micrographs of various CaO–B_2O_3–SiO_2 samples after maximum densities were achieved.

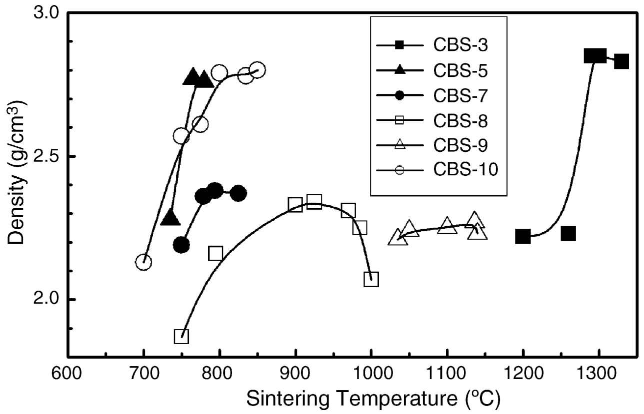

Fig. 4. The sintering densities of various CaO–B_2O_3–SiO_2 glass–ceramics.

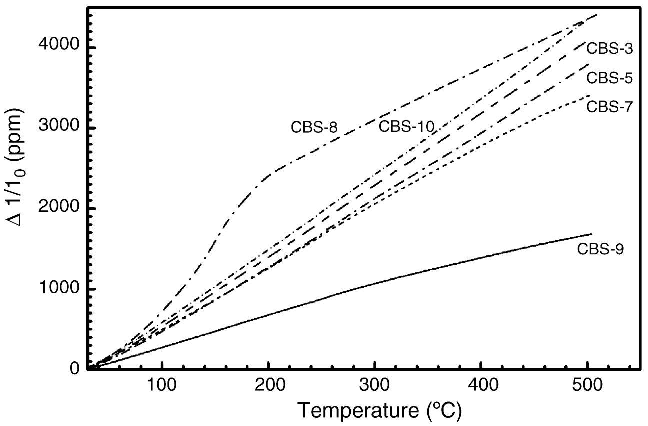

Fig. 6. Thermal expansions vs. temperature for the various glass–ceramics after densification.

various systems after maximum density were obtained. The sintering temperatures required to achieve maximum bulk density are coincidence with the shrinkage behaviors shown in Fig. 2. The maximum bulk densities are ranging from 2.3 to 2.9 g/cm^3. CaO-rich systems including CBS-3, CBS-5, and CBS-10 systems possess higher theoretical densities. SiO_2-rich systems including CBS-7, CBS-8, and CBS-9 are expected to have lower densities, particularly, for CBS-9 which only consists of SiO_2 (quartz structure) after sintering (Fig. 5). Coincide to the results shown in Fig. 2, CBS-3 densifies at the highest sintering temperature (1300 °C) with the evolution of $Ca_{11}Si_4B_2O_{22}$ and $CaSiO_3$ phases. CBS-5 and CBS-10 achieved the maximum density at 775 and 800 °C, respectively. CBS-5 remains amorphous at 780 °C and CBS-10 produces some crystalline phase of $CaSiO_3$ when they were densified. CBS-8 has a small mount of cristobalite SiO_2 phase in the early stage of densification (795 °C). Coexistence of cristobalite SiO_2 and trace $CaSiO_3$ are found when maximum densification was attained. CBS-9 densified with simultaneous formation of quartz SiO_2 phase in the glass matrix.

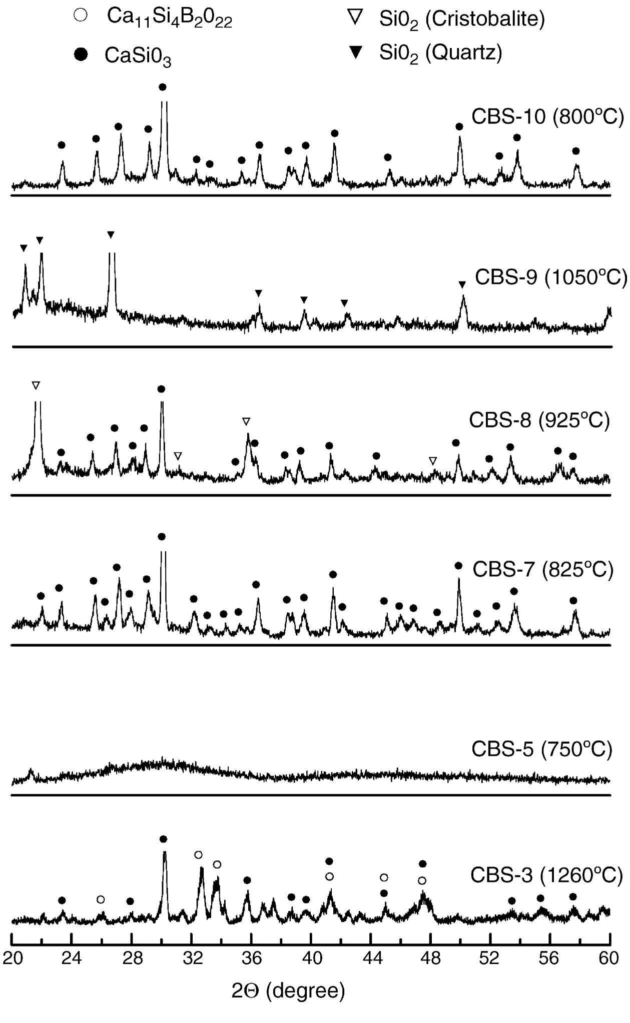

Fig. 5. XRD patterns of various CaO–B_2O_3–SiO_2 systems after maximum density were obtained.

The linear dimensional changes with temperature for various glass–ceramics are shown in Fig. 6 and the coefficients of thermal expansion (CTE) averaging from 50 to 500 °C are listed in Table 2. The dimensional changes for all system, except CBS-8, show almost linearity with temperature. There is an abrupt change in slope for CBS-8 system at ≈200 °C, which is corresponding to the phase change of SiO_2 cristobalite phase. The displacive transformation from the low cristobalite phase to the high cristobalite phase leads to the discontinuity in the thermal expansion [5]. The CTEs of the glass–ceramic systems are ranging from 3.5 to 9.7 ppm/°C, similar to those of gallium-arsenide and silicon. CBS-10 glass ceramic possesses the highest CTE and CBS-9 glass–ceramic, containing the largest amount of quartz SiO_2 phase among the various compositions studied, has the lowest CTE. The temperatures of displacive transformation for quartz and cristobalite phases are at 573 and 200–270 °C, respectively [17], that is why CBS-8 encounters discontinuity in thermal expansion in the temperature range of the CTE measurement, but CBS-9 not.

Table 2 also shows the dielectric properties of various CaO–B_2O_3–SiO_2 glass–ceramics. The dielectric constants can be divided into two groups including around 4–5 and 7–8, and the dielectric losses (tan δ) are all below 0.005 in the frequency of ≈10 GHz. The CaO-rich systems, including CBS-3, CBS-5, and CBS-10 glass–ceramics, are expected to have a higher dielectric constant, due to the polarizability of the Ca^{2+} ions

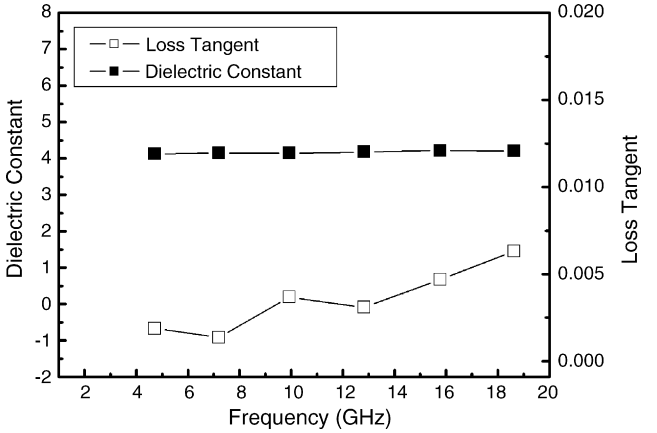

Fig. 7. Dielectric constants and dielectric losses vs. frequency for CBS-9 glass–ceramic.

(3.16 Å^3), which are much higher than those of Si^{4+} (0.87 Å^3) and B^{3+} (0.05 Å^3) ions [18]. The SiO$_2$-rich glass–ceramics, such as CBS-7, CBS-8, and CBS-9, are expected to possess lower dielectric constants since the dielectric constant of SiO$_2$ is the lowest among the ceramics. Particularly, most glass–ceramics in this study contain CaSiO$_3$ phase which has a low dielectric constant of $\approx$5. Tan δ of glass is dependent on a variety of factors. At least three types of dielectric losses for glasses have been distinguished: resonance-type vibrational losses at very high frequency, migration losses caused by the movement of mobile ions (mainly Na$^+$), and deformation losses by defect or deformation of the basic silicon oxide network [19]. Resonance-type vibrational losses are particularly important in the microwave region. Among the glasses, silica glass has the lowest tan δ in the microwave region. Although the loss level is attractive, silica is not a low-temperature co-firable ceramic if used alone. To lower the melting point, the rigid bonds in SiO$_2$ may be broken by modifiers, particularly alkali ions, but results in higher losses. It is expected that the CBS-9 would be the best in term of dielectric loss, since CBS-9 is rich in SiO$_2$ content. The dielectric constants and dielectric losses are generally frequency dependent. Typical example is shown in Fig. 7 for CBS-9 glass–ceramic. The dielectric constant increases very slightly (1.7%) while the dielectric loss raises nearly 250% as frequency increased from 4.7 GHz to 18.6 GHz (4.13 and 0.0018 at 4.7 GHz, and 4.20 and 0.0063 at 18.6 GHz). The low dielectric constant provides an attractive feature for minimizing cross-talk and increasing signal transmission speeds. The temperature coefficient of dielectric constant (TCε) for various CaO–B$_2$O$_3$–SiO$_2$ glass–ceramics listed in Table 2 indicated that the changes in dielectric constant with temperature (TCC) for the glass–ceramics are all less than 1.4% based on the measurement at 10 kHz, as also plotted in Fig. 8. The calculated temperature coefficients of dielectric constant (TCε) based on the equation of $(\varepsilon_T - \varepsilon_{25\,°C})/T\varepsilon_{25\,°C}$ are listed in Table 2. It is expected that the TCε will reduce significantly as the frequency increase since the space charge and ionic polarizations would disappear at microwave frequency. The temperature stable behavior of the CaO–B$_2$O$_3$–SiO$_2$ glass–ceramics meets the requirement for LTCC substrate applications.

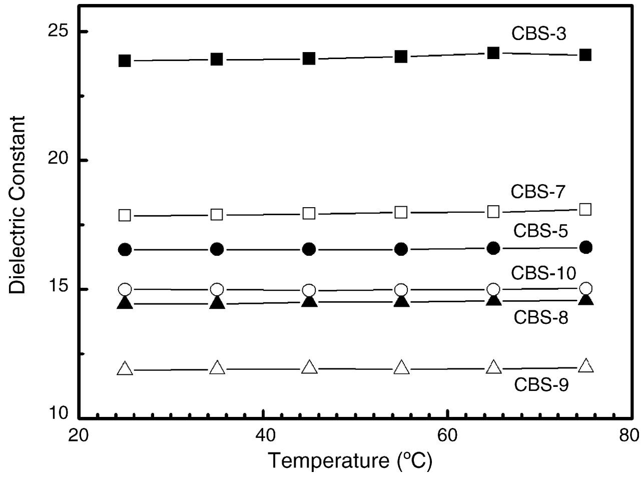

Fig. 8. Change in dielectric constant with temperature for various glass–ceramics.

It can be concluded that each constituent in the glass composition is crucial to the crystallization, densification, and thus microwave dielectric properties. However, their effects are intercorrelated and, sometimes, unable to distinguish the contributions from an individual constituent. Higher SiO$_2$ favor the formation of wollastonite (CaSiO$_3$) associated with crystallization of cristobalite, tridymite or quartz, depending on the sintering temperatures and the cooling rate, such as CBS-8 (61.7 wt% SiO$_2$). When SiO$_2$ exceed 65 wt%, wollastonite formation is prevented (CBS-9). The substrates with high SiO$_2$ content tend to possess a lower thermal expansion coefficient and lower dielectric constant at microwave frequency.

Roles of the B$_2$O$_3$ in the glass are to facilitate the vitrification and lower the melting point of the glass. The content of the B$_2$O$_3$ is limited at a maximum value of $\approx$35 wt% in this study, since it is detrimental to the resistance of acid and humidity erosion, as reported in the literature. Comparing CBS-5 and CBS-10, devitrification becomes difficult and formation of wollastonite is limited after heat treatment for glass with high B$_2$O$_3$ content.

Addition of CaO in the samples increases the melting point of the samples and makes the vitrification difficult. The higher the CaO content in the samples, the higher the firing temperature for densification and the dielectric constant is. CBS-3 is a typical example for the glass–ceramic with high CaO content.

4. Summary

In this study, the effects of the compositions of CaO–B$_2$O$_3$–SiO$_2$ glass–ceramics on the thermal behavior and microwave dielectric properties were investigated. The results indicate that most glass softening points are ranging from 680 to 710 °C, except CBS-3 at 830 °C. The level of the sintering shrinkage is correlated to the locations of the glass softening point and the crystallization point. CBS-3, containing rich CaO, has the highest onset temperature of the shrinkage and the smallest dimensional change. The maximum sintered bulk densities are ranging from 2.3 to 2.9 g/cm^3. There is an abrupt change in slope of thermal expansion for CBS-8 system at ≈200 °C, due to the displacive transformation of the high temperature and the low-temperature SiO_2 cristobalite phase. The dielectric constants can be divided into two groups including around 4–5 and 7–8, and the dielectric losses (tan δ) are all below 0.005 in the frequency of ≈10 GHz.

Acknowledgement

This work is supported by National Science Council of Republic of China (NSC-94-2216-E-027-006), which is gratefully appreciated.

References

[1] M. Valant, D. Suvorov, Glass-free low temperature cofired ceramics: calcium germanates, silicates and tellurates, J. Eur. Ceram. Soc. 24 (2004) 1715–1719.

[2] A.A. Shapiro, N. Kubota, K. Yu, M.L. Mecartney, Stress testing of a recrystallizing $CaO–B_2O_3–SiO_2$ glass ceramic with Ag electrodes for high frequency electronic packaging, J. Electronic Mater. 30 (4) (2001) 386–390.

[3] J.H. Jean, T.H. Kuan, Compositional design and properties of a low K silica dielectric for multilayer ceramic substrate, Jpn. J. Appl. Phys. Soc. 34 (4A) (1995) 1901–1905.

[4] J.H. Jean, J.I. Shen, Binary crystallizable glass composite for low-dielectric multilayer ceramic substrate, Jpn. J. Appl. Phys. Soc. 35 (7) (1996) 3942–3946.

[5] J.H. Jean, R.L. Chang, C.R. Vhang, Crystallization and properties of a low K glass composite, Jpn. J. Appl. Phys. Soc. 34 (2A) (1995) 572–577.

[6] J.H. Jean, Y.C. Fang, S.X. Dai, D.L. Wilcox, Devitrification kinetics and mechanism of $K_2O–CaO–SrO–BaO–B_2O_3–SiO_2$ glass–ceramics, J. Am. Ceram. Soc. 84 (6) (2001) 1354–1360.

[7] M.F. Zawrah, E.M.A. Hamzawy, Effect of cristobalite formation on sinterability, microstructure, and properties of glass/ceramic composites, Ceram. Int. 28 (2002) 123–130.

[8] J.H. Jean, Crystallization of boric acid on low K glass + ceramic green tapes, Jpn. J. Appl. Phys. Soc. 35 (4A) (1996) L429„L431.

[9] C.L. Lo, J.G. Duh, B.S. Chiou, W.H. Lee, Low-temperature sintering and microwave dielectric properties of anorthite-based glass–ceramics, J. Am. Ceram. Soc. 85 (9) (2002) 2230–2235.

[10] C.L. Chen, W.C.J. Wei, A. Roosen, Wetting, densification and phase transformation of $La_2O_3/Al_2O_3/B_2O_3$-based glass–ceramics, J. Eur. Ceram. Soc. 26 (2006) 59–65.

[11] S.H. Wang, H.P. Zhou, L.H. Luo, L. Qiao, Low dielectric and high frequency glass–ceramic in the system $CaO–B_2O_3–SiO_2$, Key Eng. Mater. 224–226 (2002) 31–32.

[12] S.H. Wang, H.P. Zhou, Densification and dielectric properties of $CaO–B_2O_3–SiO_2$ system glass ceramics, Mater. Sci. Eng. B 99 (2003) 597–600.

[13] C.R. Chang, J.H. Jean, Crystallization kinetics and mechanism of low-dielectric, low-temperature, cofirable $CaO–B_2O_3–SiO_2$ glass ceramics, J. Am. Ceram. Soc. 82 (7) (1999) 1725–1732.

[14] E.M. Levin, C.R. Robbins, H.F. Mcmurdie, Phase Diagrams for Ceramists, vol. 1, The American Ceramic Society, 1958„ p. 224.

[15] N. Damaskos, B.J. Kelsall, Cavity techniques for substrate properties at microwave millimeter-wave band, Microwave J. 46 (12) (2003) 112–124.

[16] C. Siligardi, M.C. Darrigo, C. Leonelli, Sintering behavior of glass–ceramic frits, Am. Ceram. Soc. Bull. (2000) 88–92.

[17] K. Kata, Y. Shimada, H. Takamizawa, Low dielectric constant new materials for multilayer ceramic substrate, in: Proceedings of the III Transaction on CHMT, vol. 13, no. 2, 1990, pp. 448–451.

[18] R.D. Shanon, Dielectric polarizability of ions in oxides and fluorides, J. Appl. Phys. 73 (1) (1993) 348–366.

[19] T. Takada, S.F. Wang, S. Yoshikawa, S.J. Jang, R.E. Newnham, Effect of glass additions on $BaO–TiO_2–WO_3$ microwave ceramics, J. Am. Ceram. Soc. 77 (1994) 1909–1916.